

## Semi-automatic mapping of cultural heritage from airborne laser scanning data

ØIVIND DUE TRIER

Norwegian Computing Center<sup>1</sup>

LARS HOLGER PILØ

Oppland County Administration<sup>2</sup>

HANS MARIUS JOHANSEN

Sør-Trøndelag County Authority<sup>3</sup>

### ABSTRACT

This paper describes semi-automatic methods for detailed mapping of some types of archaeological structure from airborne laser scanning data in Norway. The archaeological structures include point or circular features like: (1) pitfall traps in hunting systems, (2) charcoal burning pits in iron extraction sites, (3) grave mounds, either individual or in grave fields, and (4) charcoal kilns. We report on the results of using the methods for detailed mapping of Norway's largest Viking grave field at Vang, Oppdal municipality in Sør-Trøndelag County; and for detailed mapping of charcoal kilns at Lesja iron works in Oppland County.

The perceived success of using automatic detection methods depend on many factors. The most important seems to be how well the archaeological structures of interest stand out from the terrain in the DTM of the ALS ground points. We have experienced that archaeological pits in the form of pitfall traps in hunting systems and charcoal burning pits in iron extraction sites tend to stand out very well. Natural pits of the same shape and size are rare in Norwegian landscapes. On the other hand, grave mounds are more easily confused with natural terrain features. The grave mounds have

---

1 Section for Earth Observation, Gaustadalléen 23A, P.O. Box 114 Blindern, NO-0314 Oslo, Norway. Email: trier@nr.no. Website: <http://earthobs.nr.no>.

2 Section for Cultural Heritage Management, P. O. Box 988, NO-2626 Lillehammer, Norway. Email: Lars.Holger.Pilo@oppland.org.

3 Department of Regional Development, Section for Area and Environment, P.O. Box 2350 Sluppen, NO-7004 Trondheim. Email: hans.marius.johansen@stfk.no.

a less distinct shape than the archaeological pits, many grave mounds are distorted, and there are many natural (partially) mound-like terrain features.

Although far from perfect, automatic detection is now used as part of the standard routine in detailed archaeological mapping in Vestfold and Oppland Counties. The current perspective is that automatic detection will not replace archaeologists, but is a useful tool for archaeologists in detailed mapping of cultural heritage. Our goal is to provide semi-automatic detection methods that are used by all 19 counties in Norway for detailed mapping of cultural heritage.

**Keywords:** Lidar, Grave mound, Charcoal kiln, Iron works, Iron Age, Viking.

## 1. INTRODUCTION

Several Norwegian municipalities are experiencing growing pressure on agricultural and forested land for development, being it new residential areas, new mountain cabins and hotels, new highways, or other purposes. The traditional mapping of cultural heritage, mainly based on chance discovery and with inaccurate positioning, has proven inadequate for land use planning. Therefore, the Norwegian Directorate for Cultural Heritage (in Norwegian: Riksantikvaren), in cooperation with three Norwegian counties (Vestfold, Oppland and Sør-Trøndelag), the Museum of Cultural History at the University of Oslo, and the Norwegian Institute for Cultural Heritage Research, are investing in the development of new methods, using new technology, for a more systematic mapping of cultural heritage.

A project was started in 2002 by the Norwegian Directorate for Cultural Heritage, aiming at developing cost-effective methods for surveying and monitoring cultural heritage on a regional and national scale. During the first years, the focus was on the automatic detection of crop marks and soil marks in cereal fields in satellite and aerial images (Aurdal *et al.*, 2006; Trier *et al.*, 2009). Several of these detections have been confirmed to be levelled grave mounds, dating to 1500-2500 years ago.

However, methods based on optical images are of limited value in forested areas, since the archaeology tends to be obscured by the tree canopies. However, by using airborne laser scanning (ALS) data, the forest vegetation can be removed from the data, making it possible to detect archaeology in a semi-automatic fashion, provided the archaeology manifests itself as details in the digital terrain model (DTM) of the ALS ground returns (Figure 1), and that these details may be described by some pattern.

For visual inspection of a DTM, a number of visualization methods exist, including the standard hill-shading and slope images, which are available in many software packages like ENVI and ArcGIS; sky-view factor (Kokalj *et al.*, 2011) and local relief models (Hesse, 2010). Some of the lidar visualisation techniques are available in the LiDAR Visualisation Toolbox (LiVT) at <http://www.arland.eu/outreach/software-tools>. Several authors have mapped cultural heritage by visual inspection (e.g., see (Bewley *et al.*, 2005), (Bollandsås *et al.*, 2012)). However, given the vast amounts of data generated by ALS,

semi-automatic detection methods are needed to assist visual interpretation of the ALS data. If successful, this may lead to more targeted and less time-consuming field work.

So far, the project has developed methods for the automatic detection of pit structures (Trier and Pilø, 2012) and mound structures (Trier *et al.*, 2015). Automatic pit detection may be used in semi-automatic detection of hunting systems and iron extraction sites, and automatic mound detection may be used in semi-automatic detection of grave mounds. Currently, we are developing semi-automatic detection of charcoal kilns. We also plan to develop semi-automatic detection of linear structures like hollow ways and stone fences.

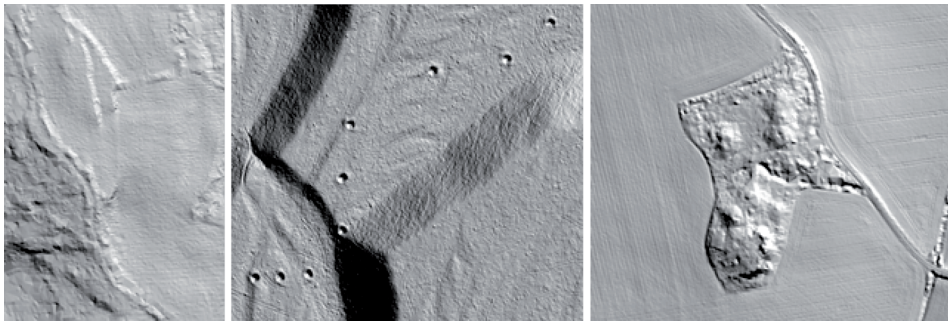


**Figure 1.** Airborne laser scanning (ALS) data from some Norwegian municipalities. Left: Kongsberg, with stone fences. Middle: Nord-Fron, with pitfall traps for moose hunting. Right: Larvik, with grave mounds.

The rest of the paper is organized as follows. Section 2 outlines the general detection method. Section 3 describes semi-automatic mapping of Norway's largest Viking grave field. Section 4 describes semi-automatic mapping of charcoal kilns at Lesja. Section 5 discusses the current status and future possibilities of semi-automatic detection of cultural heritage in Norway, and gives some conclusions.

Many of the illustrations in this chapter are superimposed on base maps from the Norwegian Mapping Authority (In Norwegian: Statens Kartverk).

## 2. GENERAL APPROACH FOR SEMI-AUTOMATIC DETECTION OF CIRCULAR ARCHAEOLOGICAL STRUCTURES

The main purpose of the semi-automatic detection methods is to facilitate a more complete and accurate mapping of cultural heritage, while at the same time to reduce the human effort needed for this purpose. The method requires that ALS data be collected for the area of interest, with a recommended minimum ALS pulse density of  $5/m^2$  (Trier and Pilø, 2012). Since deciduous trees with leaves fully developed are known to block the ALS pulses from reaching the ground, ALS data collection in the leaf off seasons is

recommended. In Norway, this may be a challenge in terrains with large elevation differences, since leaves on deciduous trees may be quite developed in lower elevations, while at the same time, the ground may be partly snow covered in higher elevations. One possible solution is to collect ALS data on several dates, but this may increase the ALS data collection cost.

The automatic method has the following steps:

1. Pre-processing: convert ALS point data to a digital terrain model (DTM) of the ground surface (without vegetation).
2. Template matching using templates of varying sizes
3. Merge overlapping detections
4. Measure various deviations from an ideal shape
5. Estimate a confidence score for each detection

## 2.1. Pre-processing

The purpose of the pre-processing is to convert the ground returns of the ALS point cloud data to a rectangular image grid (in this case a DTM), to allow for subsequent image processing methods. The pixel size of the DTM is a compromise between the need to keep all the detail of the point cloud data while at the same time to limit the processing time needed for template matching. For a given geographical area, the execution time of the template matching step is proportional to  $n^4$ , when the template size is  $n \times n$  pixels. This fact makes it attractive to use multiple DTM resolutions, to limit the template size in pixels, and thus to limit the execution time.

## 2.2 Template matching

Template matching by image correlation (Gonzalez and Woods, 1992, pp. 583-585) is used to find locations in the DTM that may be cultural heritage structures of a specific shape. So, if more than one shape of structure is sought, then a template for each shape be constructed. Further, each template shape must be reproduced in different sizes, covering all the expected sizes of the specific shape.

For one specific size of specific template applied at one specific resolution of the DTM, the result is an image which has several local maxima. Each local maximum represents one template match. A quick way to locate the local maxima is to threshold the correlation image and then to find the maximum within each region. However, there is a trade-off here: if a too low threshold is used, then several strong local maxima may be merged into one region; while if a too high threshold is used, then only a few local maxima may be found. So, if the final detection result seems to miss several visually clear structures of the desired kind, then one may inspect the thresholded correlation image to understand if the threshold may be too low or too high, or if a more elaborated local maximum detection method is needed.

### 2.3. Merging overlapping detections

A typical result of the template matching step is that one structure in the DTM may give a good match at several template sizes, resulting in a number of concentric detections. These need to be eliminated, keeping only the strongest. However, we have also seen examples of one or a few small grave mounds located on top of a big grave mound, so this must also be allowed for when constructing rules for eliminating overlapping detections.

### 2.4. Measuring various deviations from an ideal shape

While the template matching step may be good at finding structures in the DTM that resemble the shape of the template, the template matching step may also find other structures that deviate quite much from that shape. This may happen if the true archaeological structures have quite large deviations from the ideal shape. Therefore, one may use additional geometric measurements of the shape of each detected structure. For heaps, we have used (Trier *et al.*, 2015):

1. Root-mean-square (RMS) difference of template and detection. For this purpose, a sub-image of the detection is normalized to have zero average height, the same size, and the same height difference between the interior and the circular edge as the template.
2. Minimum height, measured as the height difference between the highest point inside the mound detection and the highest point on the ring edge.
3. Average height, measured as the height difference between the highest point inside the mound detection and the average height on the ring edge outside the mound.
4. Minimum height divided by radius, which we call normalized minimum height.
5. Average height divided by radius, which we call normalized average height.
6. Squared gradient
7. Standard deviation of gradient
8. Gradient
9. Normalized convolution.

The motivation for using the gradient in some of the measurements is that some of the false detections are natural terrain features with one or more very steep sides.

For pits, we used (Trier and Pilø, 2012):

1. Normalized convolution
2. Minimum depth
3. Average depth
4. RMS difference
5. RMS difference with an alternative pit template more resembling an eroded pit
6. Offset
7. Elongation

Offset and elongation were computed as follows. For each pit, a threshold is defined as the value that separates the pixels inside the pit into two groups, the 25% of the pixels that are lower than the threshold, and the 75% that are higher. Use this threshold to extract the shape of the pit from a square image centred on the pit, with sides equal to six times the radius. From the extracted pit shape (Figure 2), the offset and elongation are computed.

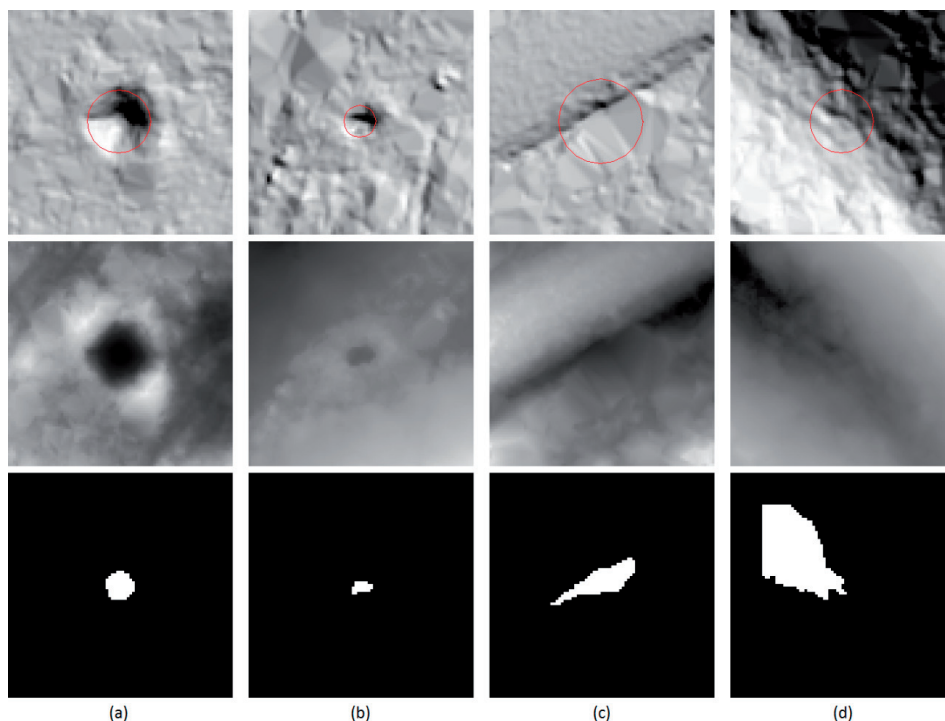


**Figure 2.** Extraction of pit shape for computation of elongation and offset. Top: hill-shaded relief of DTM with pit detections superimposed as red circles. Middle: DTM with local contrast enhanced for each subimage. Bottom: extracted pit shapes. (a) Pitfall trap. (b) Small pitfall trap. (c) Ditch along road edge. (d) Natural valley.

## 2.5. Confidence score

Since the template matching step may result in a very large number of detections, even after the merging step, it is useful to rank the detections so that the strongest and most likely detections are labelled as such, and the weakest and less likely detections are labelled differently. A confidence score 1-6 is used for this purpose, and rules for assigning confidence scores may be constructed from training data with confirmed archaeological structures. The confidence scores may be computed by using *if*-tests on the measurements in the previous step. By grouping detections with the same confidence level in a separate GIS layer, they may be switched on and off for visual inspection of the detection results.

### 3. SEMI-AUTOMATIC MAPPING OF THE IRON AGE GRAVE FIELD AT VANG, OPPDAL

The grave field at Vang, Oppdal municipality, Sør-Trøndelag County, is the largest Iron Age burial site in Norway and one of the most extensive in Northern Europe. More than 800 mounds and cairns are built within 42 acres (168 000 m<sup>2</sup>). They are built alongside, on top of, and intertwined with each other. The grave field is located 2 km west of Oppdal town centre, south of highway 70 (Figure 3). The grave field is maintained as a cultural heritage park.

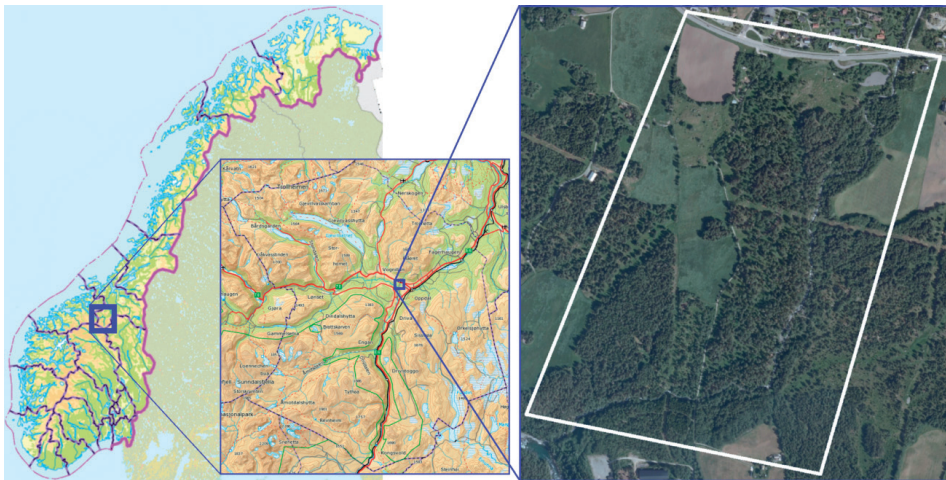


**Figure 3.** Location of ALS data. Left: map of Norway, with county boundaries. Middle: map of Oppdal municipality in Sør-Trøndelag County. Right: orthophoto of a small part of Oppdal municipality, with the ALS data extent superimposed in white.

The existing mapping of the grave field is inaccurate and has some mistakes. The individual grave mounds need to be mapped accurately and entered into the Norwegian national cultural heritage database Askeladden. Also, the existing information signs are to be replaced with new signs based on the new mapping.

The norm in the Iron Age was for each farm to maintain a separate burial ground. In Oppdal, the practice of large communal burial grounds appears to have been the norm. Such burial grounds have been located on three sites in Oppdal. Today the grave field at Vang is the only preserved site.

Mounds from the Viking Age are dominant at Vang (Figure 4). The common shape is circular with a diameter between 2 and 20 meters. The height of the mounds varies from low and almost bashful to tall and large up to at least 3 m. Some mounds (<10%) are oblong in shape. Artefacts found in such graves at Vang and elsewhere in Norway show that these long barrows are almost always female graves.

The burials from the Migration Period consist of circular and flat stone cairns with a diameter up to 3-4 meters (Figure 5). Between the mounds are unknown amounts of flat graves, where the dead were buried in a pit in the ground, unmarked and not visible from the surface.



Figure 4. Grave mounds from the Viking Age (800-1000 AD) at Vang, Oppdal municipality.



Figure 5. Grave cairn from the Migration Period (400-600 AD).



Archaeological digs were conducted on 10 mounds in 1966-1990 (Farbregd, 1980; 1993). These burials were all dating back to the Viking Age (800-1000 AD), but some artefacts and structures were dated back to around 500 AD as well.

2 grave cairns were excavated in 1999 (Fløttum, 2004). Both contained remains of earthenware from the Migration Period (400-600 AD), an evidence of Vang being used as burial ground since the Early Iron Age.

### 3.1. Data

The existing archaeological map was surveyed in 1936 and 1967 (Farbregd, 1980). A few of the grave mounds have been excavated (Farbregd, 1993).

Airborne laser scanning (ALS) data was collected for a 0.63 km<sup>2</sup> area, covering the known grave field at Vang, Oppdal municipality, Sør-Trøndelag County, Norway (Figure 3). Data was collected on 12 September 2012 by the commercial provider TerraTec AS, Norway, using a Leica ALS70 laser scanner mounted on an aircraft flying at 150 knots and 589 m maximum elevation above the terrain. The specified point density was 12/m<sup>2</sup>. Each pulse may result in up to four discrete returns. Each recorded return was stored with the return number (1-4), intensity, (x, y, z) position, and a class label (Table 1).

**Table 1**  
Class labels for ALS data

class	description
1	undassified
2	ground
7	noise
9	water
10	bridge

For the purpose of method development, the ALS data has been divided into a training data set and a test data set (Figure 6).

### 3.2. Detailed mapping of grave mounds

Detailed mapping of each grave mound was done by digitizing a circle or ellipse, with the following as backdrops that could be switched on and off (Figure 7):

1. Aerial orthophoto (only useful in open terrain without trees and tree shadows)
2. Hill-shaded terrain, generated from ALS ground points
3. Local relief model (Hesse, 2010), also generated from ALS ground points
4. Automatic detections, with one separate layer for each confidence level 1-6.

In addition, the existing archaeological map was used as reference.

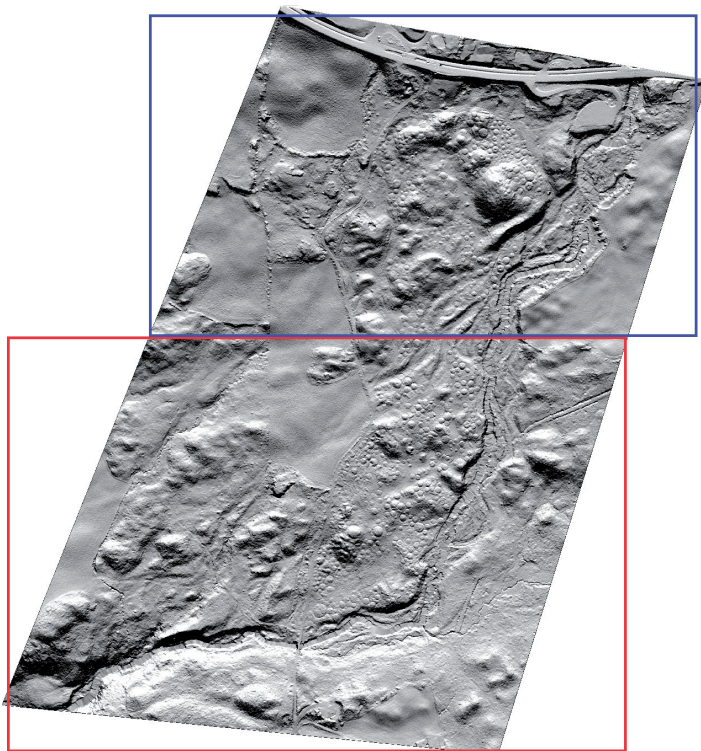


Figure 6. Division of ALS data into training data (blue) and test data (red).

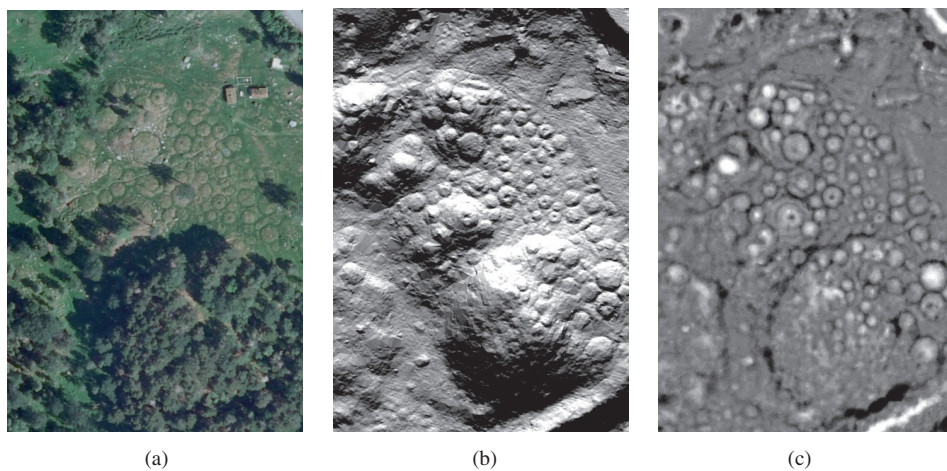


Figure 7. Detail of a part of the grave field. Left: aerial orthophoto. Middle: hill-shaded relief of DTM. Right: local relief model.

### 3.3. Automatic mapping of mound structures

We have previously developed methods for the semi-automatic detection of archaeological pits (Trier and Pilø, 2012) and grave mounds (Trier *et al.*, 2015). For the grave field at Vang, we observed that many grave mounds were located on hillsides, i.e., on slopes. However, the grave mound templates are developed for grave mounds in flat terrain. The local relief model (Hesse, 2010) is removing the general shape of the terrain, thus emphasizing local terrain variations caused by grave mounds but also other terrain features of the same scale.

A number of visualisation techniques have been proposed for DTMs. The default visualisation is to use a hill shaded relief (Figure 7b), which is very intuitive, but has a number of drawbacks. First, the use of a directional light source precludes detail parallel to this direction from being visible. Second, details may be hidden in shadows, and third, this visualisation method is not suitable as input to automatic detection. Alternative visualisation methods include gradient image, local relief model (Hesse, 2010), sky-view factor (Kokalj *et al.*, 2011), and openness (Doneus, 2013). The local relief model results in visualisations that are intuitive (Figure 7c), and at the same time suitable for subsequent automatic processing.

We have constructed mound templates from the grave mounds in the training data (Figure 6). For each mound, the centre position and radius was measured manually in the local relief model. Then, for each mound, a square sub-image was constructed, with side length equal to  $4 \times$  radius. Each sub-image was scaled to the same size,  $100 \times 100$  pixels, which is  $20 \text{ m} \times 20 \text{ m}$  at  $0.2 \text{ m}$  pixel size. This results in  $5 \text{ m}$  radius. Since each mound was labelled as either ‘intact’ or ‘with pit’, average mounds for each of the two types were constructed, in addition to an average of all mounds.

Inspecting the average mounds obtained from the DTM and the local relief model (Figure 8), one may observe that they seem to be almost symmetric inside the heap boundary, but somewhat uneven on the outside. To construct rotationally symmetric templates, grave mound profiles were obtained by using the average height for all pixels having the same distance to the template centre (Figure 9).

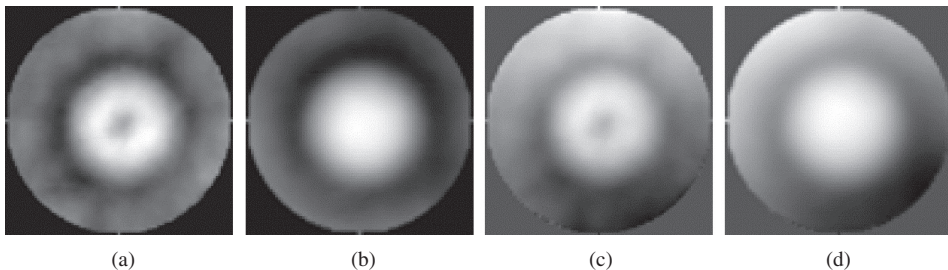


**Figure 8.** Average mound shapes extracted from training data. (a) Grave mound with pit, from DEM. (b) Intact grave mound, from DEM. (c) Grave mound with pit, from local relief model. (d) Intact grave mound, from local relief model.

By comparing the mound template profiles for intact mounds obtained from the DTM (Figure 10) with the profile for intact mounds obtained from the local relief model, we observe that the standard deviation is smaller with the local relief model. The same observation is made when comparing the mounds with pits. Therefore, we will use the local relief model as input to the automatic detection method.

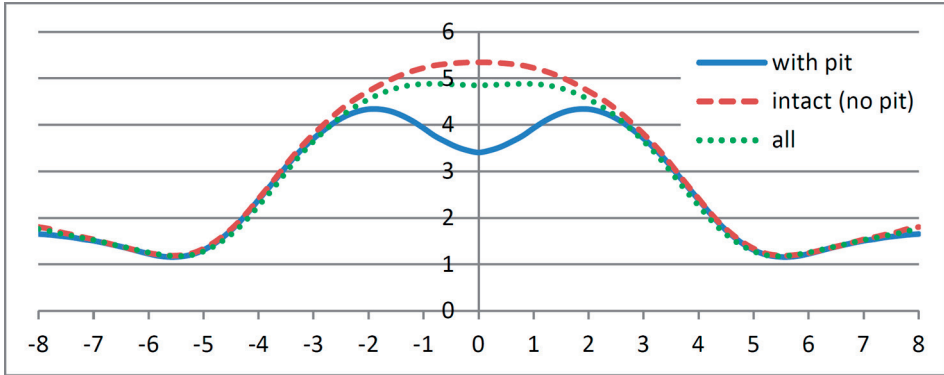


Figure 9. Profile of average grave mound shapes, from DEM of training data.

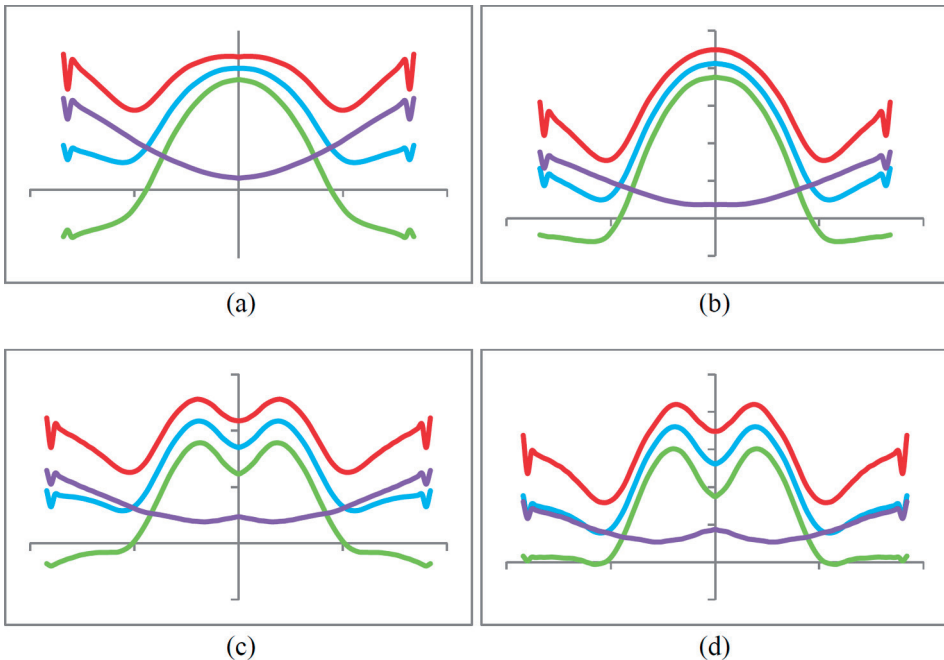


Figure 10. Average and standard deviation of profiles of grave mounds, obtained from the training data. Blue: average. Purple: standard deviation. Green: average minus standard deviation. Red: average plus standard deviation. (a) Intact grave mounds, from DTM. (b) Intact grave mounds, from local relief model. (c) Grave mounds with pits, from DTM. (d) Grave mounds with pits, from local relief model.

### 3.4. Results

The method was used on the entire lidar data set in order to provide automatic detections as backdrops for manual verification and field inspection. However, using all automatic detections is not very helpful, as the number of false positives is too high. Rather, one should start with the automatic detections with confidence high and very high (Figure 11a). The majority of these detections are true grave mounds. However, many grave mounds are also missing. By including detections with medium high and medium confidence, more grave mounds are detected (Figure 11b). However, the number of false detection increases. One may continue to include detections with low and very low confidence (Figure 11c). However, this further increases the number of false detections.

Visual inspection was done by using the existing archaeological map as a backdrop in addition to the local relief model and the hill-shaded relief. By cycling through the different backdrops, each grave mound detection was evaluated as being one of:

1. Grave mound, well preserved
2. Grave mound
3. Grave mound, elongated
4. Possible grave mound (not in the existing archaeological map, but clearly visible in the local relief model and/or the hill-shaded relief)

In addition, missing grave mounds were recorded, each being one of:

5. Missing grave mound (present in existing archaeological map but not detected by automatic method)
6. Missing elongated grave mound (as above, but elongated)
7. Missing possible grave mound (not in existing archaeological map, not detected by automatic method, but clearly visible in the local relief model and/or hill-shaded relief).
8. Missing possible elongated grave mound (as above, but elongated)

Visual inspection of the automatic detections reveals that the automatic method is able to detect the majority of grave mounds (Figure 11d). However, the exact size and shape of each grave mound has not been corrected at this stage. Of the 295 grave mounds in the training data, corresponding to the northern part of the existing archaeological map, the automatic method is able to detect 238 (81%), but misses 57 (19%). In addition 15 possible grave mounds are detected, and 10 possible grave mounds are missed (Table 2). Of the 469 grave mounds in the test set, the automatic method detects 304 (65%) and misses 165 (35%). In addition, 10 possible grave mounds are detected, while 11 possible grave mounds are missed.

Table 2

Automatic detection results in the training data (northern part of grave field) and test data (southern part of grave field), evaluated by visual inspection and compared with existing archaeological map.

Type of grave mound	training		test		total	
Grave mound, well preserved	82		105		187	
Grave mound	156		197		353	
Elongated grave mound	0		2		2	
Sum detected grave mounds	238	81%	304	65%	542	71%
Missing elongated grave mound	14		52		66	
Missing grave mound	43		113		156	
Sum missing grave mounds	57	19%	165	35%	222	29%
Sum grave mounds in existing archaeological map	295		469		764	
Possible grave mound	15		10		25	
Missing possible elongated grave mound	1		0		1	
Missing possible grave mound	9		11		20	
Sum grave mounds and possible grave mounds	320		490		810	

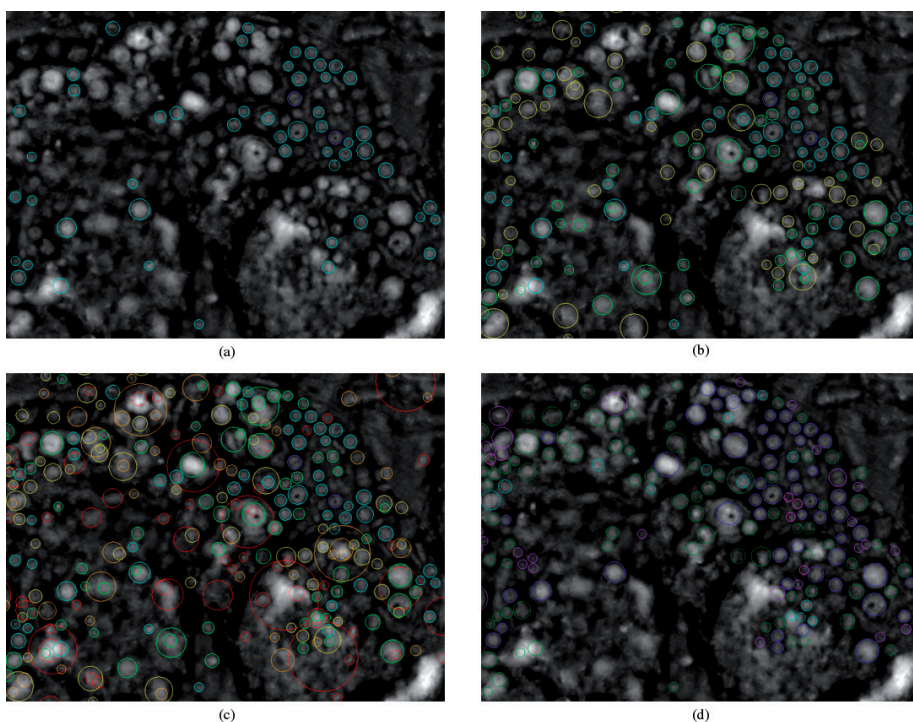


**Figure 11.** Heap detections superimposed on a local relief model of the ALS data. (a) Automatic detections (coloured circles) with very high (dark blue) and high (cyan) confidence. (b) Same as (a), plus: medium high (green), medium (yellow) confidence. (c) Same as (b), plus: low (orange) confidence, and very low (red) confidence. (d) Result of visual inspection. Blue: well preserved grave mound. Green: grave mound. Cyan: possible grave mound. Purple: missing grave mound. Pink: missing possible grave mound. Here, ‘possible’ means that the location is not marked as grave mound on the existing archaeological map, but that the visual inspection has concluded that it may be a grave mound.

The grave mounds that are detected include grave mounds with pits (Figure 12a), grave mounds located in slopes (Figure 12b), flat grave mounds (Figure 12c), and grave mounds with minor shape distortions (Figure 12d).

The grave mounds that were not detected seem to be of three major categories:

1. Long barrows, i.e., elongated grave mounds (Figure 13a) are seldom detected, due to the fact that the method is designed to find round structures.
2. Grave mounds with a distorted shape (Figure 13b).
3. Grave mounds located at abrupt terrain changes, e.g., the edge of a steep slope (Figure 13c). In such cases the local relief model is not able to separate the grave mounds from the surrounding terrain.

The automatic detections were used as input to the ongoing, detailed re-mapping of the grave field. A preliminary mapping exists, after partial field survey in the northern part. Field survey will continue in 2015. By comparing the preliminary re-mapping (Figure 14a) with the automatic mapping after visual inspection (Figure 11d), a number of differences may be observed. Some mound structures that were believed to be grave mounds after visual inspection, were not believed to be grave mounds by the preliminary re-mapping, and vice versa. Also, the exact size and shape may vary for the grave mounds that appear in both mapping results.

By overlaying the preliminary re-mapping on the existing archaeological map, the inaccuracies of the latter become evident (Figure 14b).

The re-mapping contains some grave cairns from the Migration Period (e.g., see Figure 5). These have too small elevation differences with the surrounding terrain to be visible in the DTM, and are therefore not detected by the automatic method.

#### 4. SEMI-AUTOMATIC MAPPING OF CHARCOAL KILNS AT LESJA

The history of Lesja Ironworks has been described in detail by Berg (1983, 1984, 1985, 1986) and Jakobsen (1997). A summary is given here.

The 17<sup>th</sup> century saw the establishment of a number of iron works in Norway, based on the need of the Danish king for iron for ships, armaments and other military purposes. A typical feature of such iron works was the forced labour put on local farmers to supply wood and charcoal for the mines and the furnaces. This was normally done by establishing a circumference described in a royal letter of privilege, within which the local farmers had to supply set materials at a fixed price.

The iron works at Lesja (in Norwegian: Lesja Jernverk) was established 1660 in the wake of the discovery of iron ore locally. Royal privileges were given to the owners, including the forced supply of wood and charcoal within a circumference of 40 km. Since the iron works were placed in a forested valley with bare mountains to the north and south, this supply of wood and charcoal had to be collected from the valley extending to

the southeast and northwest from the iron works. Since Lesja was a marginal agricultural settlement, the extra income from producing charcoal was welcomed by the local farmers. It is known from historical records that the local forests were cut down to such a degree already in the mid-18<sup>th</sup> century, that scarcity of charcoal put limits on the production of iron. After intermittent production of iron during the lifetime of the iron works, the production of iron at Lesja Jernverk ceased permanently in 1812.

The *Bergmeister* for such iron works as a rule came from present-day Germany, where there was already a long tradition of mining iron ore and producing iron in blast furnaces. The Bergmeister brought with them a different tradition of producing charcoal – in kilns, instead of in pits, as had been the case in Norway in the Late Iron Age and the Medieval Period.

Surveys in connection with cultural heritage management work have pointed to the presence of large numbers of charcoal kilns in the area surrounding the Lesja Jernverk. It was not known, however, what the total number of preserved kilns was, if they showed sign of reuse, and how they were distributed throughout the circumference described in the royal letter of privilege.

In 2013 the entire forested valley in Lesja was mapped with lidar by TerraTec AS, using a Leica ALS70 airborne laser scanner. The quality of the data is five first returns per m<sup>2</sup>. The initial visual interpretation of the lidar data, based on a single-light source hillshade and a spatially limited local relief model covering only the central area, yielded about 1000 possible charcoal kilns. All were round, with a diameter between 10 and 20 m. However, the edge of the kilns had a varied topographical expression. Some kilns had a ditch surrounding them, some had pits, and some had a combination of the two. In addition some kilns had a low mound inside the ditch/pits or even pits inside the circumference.

The topographical expression of the charcoal kilns combining pits, round ditches and mounds made it likely that previous work on automatic detection (Trier and Pilø, 2012; Trier *et al.*, 2015) would be applicable in the search for charcoal kilns in the data. This was confirmed by a test run of the detection of pits and mounds on the central part of the data set (Figure 15). The first step in developing an automatic detection method specifically for charcoal kilns was to collect field data for a training data set.

The fieldwork for the training set was conducted in early June 2014. Participants were Frank Røberg and Lars Pilø, Oppland County Council and Rolf Sørumgård, Lesja. The survey covered an area of 1.8 km<sup>2</sup>, just east of the iron works. The area surveyed covered terrain on both sides of the Lågen River, and was quite hilly. Nearly all recorded charcoal kilns were situated either on flat terraces or in depressions in the terrain. None were found on hilltops. This is most likely due to practical reasons: transporting timber downhill to the kilns is easier than uphill. Within the 1.8 km<sup>2</sup> survey area, the kilns identified by visual inspection were visited, but also a complete mapping of kilns was undertaken. A total of 183 kilns were recorded (Figure 16), including attribute data describing their topographical expression.





(a)



(b)



(c)



(d)

**Figure 12.** Examples of detected grave mounds. (a) 8 m wide grave mound with central pit. (b) 10 m wide grave mound in a slope. (c) Two flat grave mounds, 8 m wide (in image centre) and 7 m wide (behind). (d) 8 m wide grave mound with minor shape distortions in the form of bumps.



(a)



(b)



(c)

**Figure 13.** Examples of grave mounds that are not detected. (a) A long barrow (in image centre), 6 m long and 3 m wide; surrounded by circular grave mounds that are detected. (b) Flat grave mound (in image centre) with shape distortions in the form of bumps. The grave mounds behind it are detected. (c) Grave mound located at the edge of a steep slope.

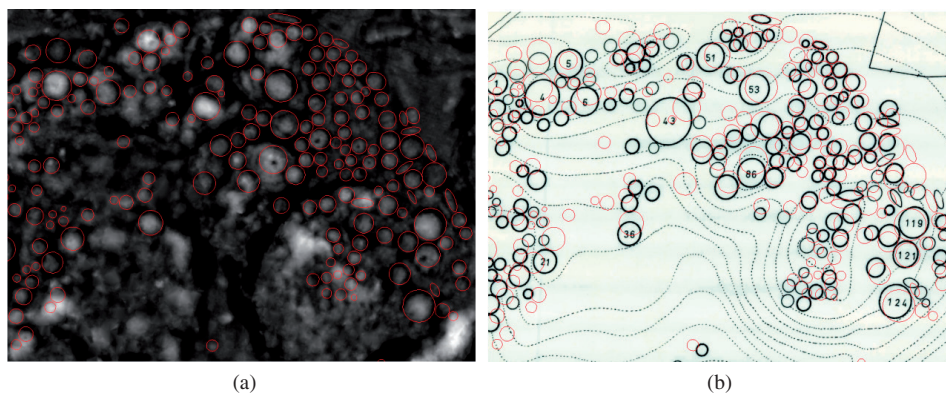


**Figure 14.** (a) Preliminary result of on-going detailed re-mapping. (b) Comparison between existing archaeological map (black) and new mapping of grave mounds (red).

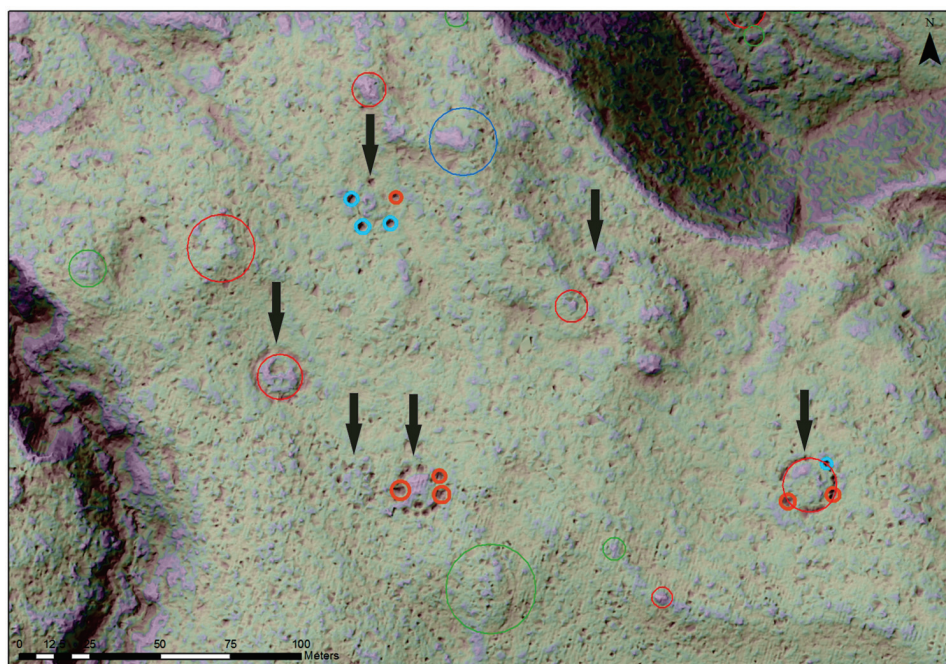


**Figure 15.** Charcoal kilns (marked with arrow), with automatic detections of pits (small circles in thick lines) and mounds (large circles in thin lines), of medium to high confidence. From the test run of automatic detection, prior to the field control.

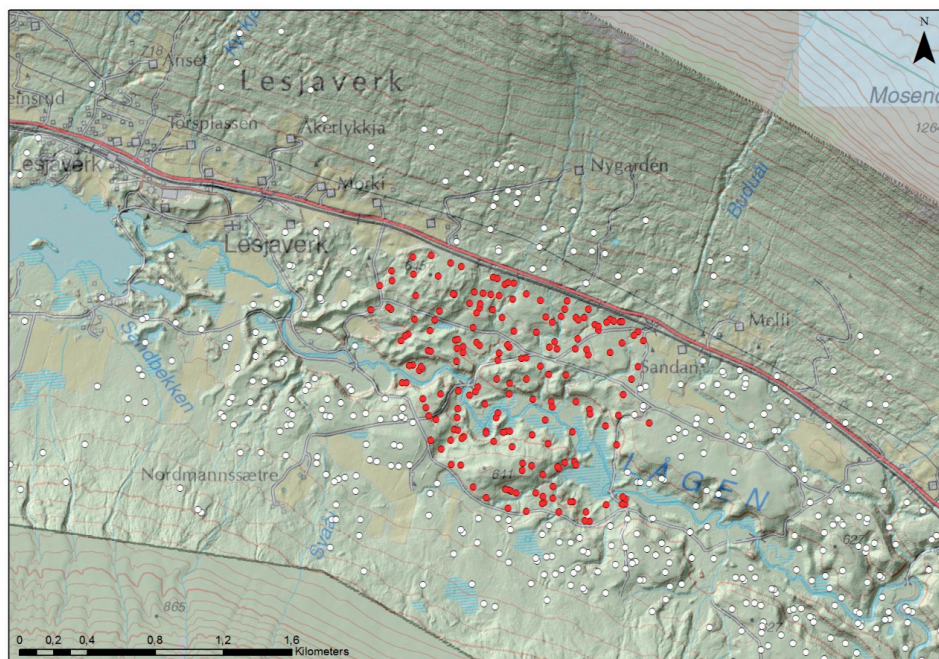


Figure 16. Charcoal kilns recorded in the field (red) and found during visual inspection of the data (white).

Based on the field control, a new visual inspection of the lidar data was undertaken. The quality of this re-interpretation was strengthened by the application of a new WMS-visualization developed by COWI and Oppland County Council (Figure 17). Using a combination of methods (local relief model, sky view factor, slope and MDOW hillshade, the parameters of which can be remotely controlled) it provides a better visualization of the lidar data, enhancing the quality of the visual interpretation.

In order to design tailored kiln detection methods, it is important to understand what types of kiln morphology are detected by automatic pit and/or heap detection, and what types are not detected. Some kilns are detected as one or more pits (Figure 18), some as one mound (Figure 19), and some as one mound and one or more pits (Figure 20). Of the kilns that are not detected at all (Figure 21), many have a fair, circular ditch along the perimeter, so an automatic circular ditch detection method may be attempted.

The new interpretation yielded a total of 905 suspected charcoal kilns (not confirmed in the field), which may also be used for training purposes.

The overall map of the distribution of charcoal kilns (Figure 22) shows some interesting features, which may or may not be an expression of the real distribution of the charcoal kilns. Most of the charcoal kilns have been found on old flood plains or glacial washout deposits. Today these plains are covered by open pine forest. This gives excellent conditions for lidar, and could imply that kilns in such topographical situations are

over-represented on the map. That this could be the case is supported by the fact that it was only discovered quite late during the first round of visual inspection, that charcoal kilns were also present in the hillside north of the iron works. They have a different topographical expression, being dug into the hillside on one side, and having a terrace on the other side – to provide a platform for the kiln. They may be difficult to spot, even using the new WMS-visualization.

One may also discuss why kilns are missing in some areas. The low number of kilns in the mining area northwest of the iron works is understandable, since the timber here would have been used for fire-setting in the mines. The lack of kilns in the old settlement area to the east of the Lora River could be caused by lack of forests in this area at the time of the iron works, since the timber here would already have been used for buildings, fences and other agricultural purposes. Lack of kilns at the mouth of the Grøna River in the north-western part of the circumference is puzzling, but may be caused by extensive flooding in the area, following the 1789 flooding catastrophe that struck much of the region.

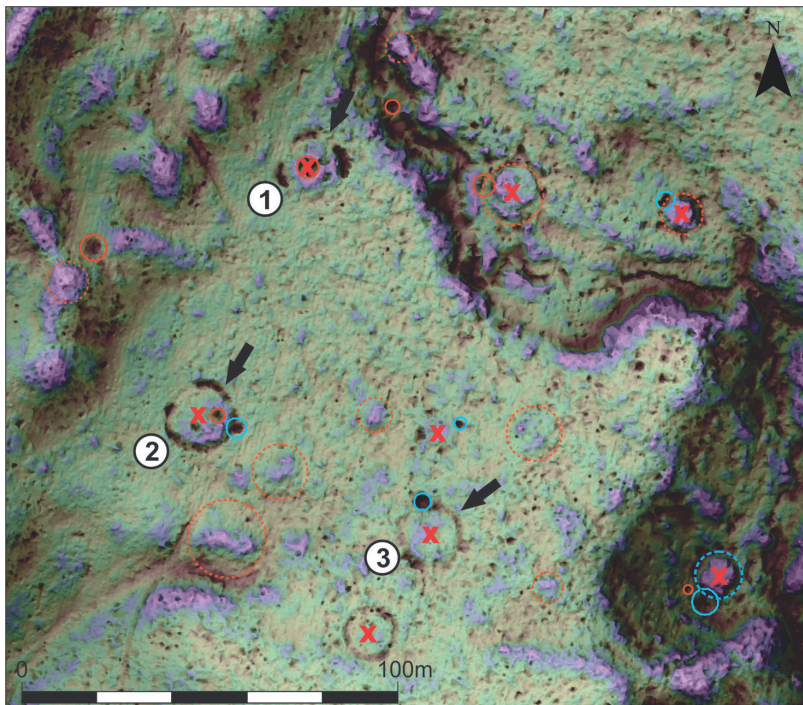


**Figure 17.** The new WMS-visualization showing the charcoal kilns clearly, using a combination of local relief model, sky-view factor and slope. Legend: red x = charcoal kiln centre, dashed circle = mound detection, solid circle = pit detection; blue circle = high confidence detection, orange circle = medium high confidence detection. Photographs of the three numbered kilns appear in Figure 18, with the viewing directions indicated with black arrows.

Future work will include further development of automatic detection of charcoal kilns based on the 2014 training data set, performed on the entire lidar data set from Lesja. Based on this improved detection method, targeted fieldwork will address the problems of the representativity of the distribution map described above.

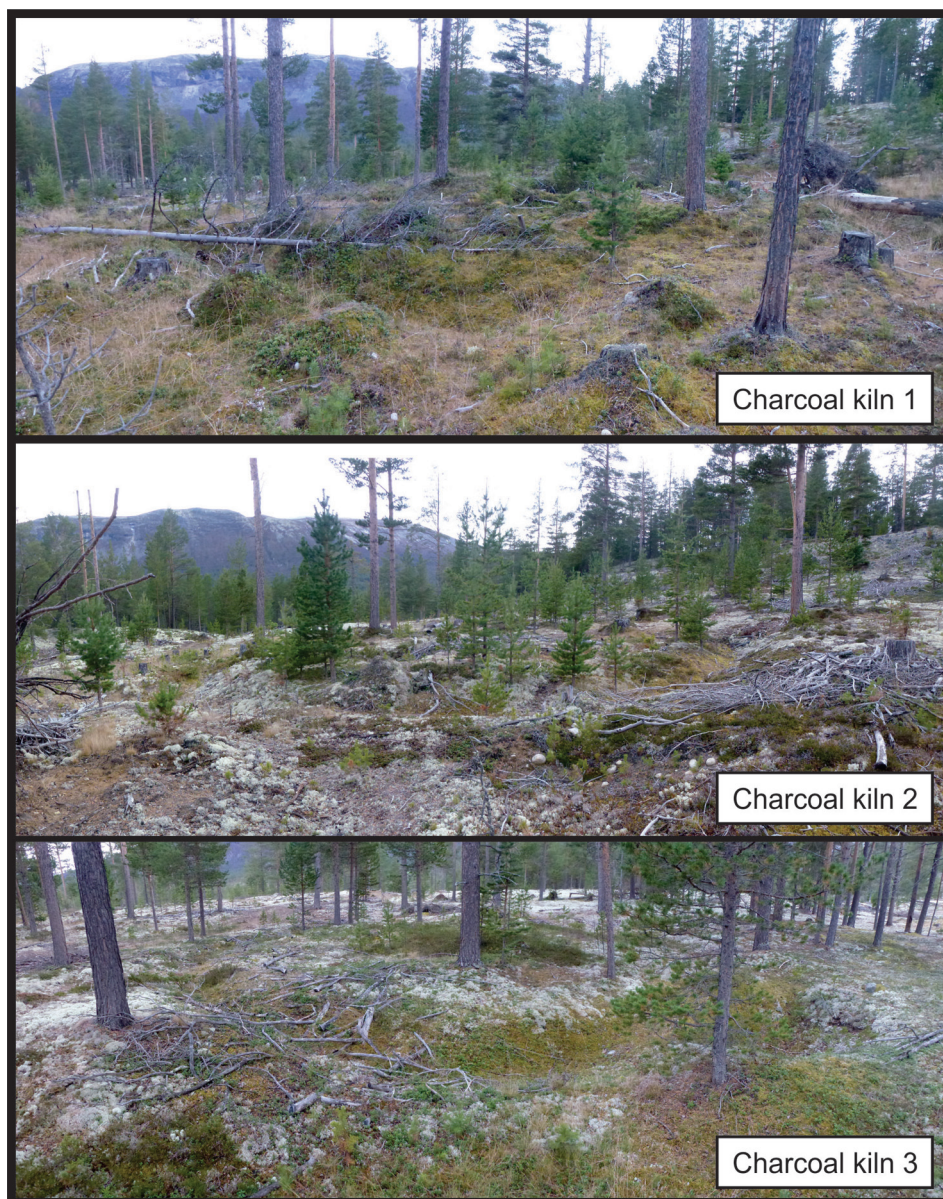


Figure 18. Examples of charcoal kilns in Figure 17 that were found by automatic pit detection.



**Figure 19.** A charcoal kiln that is detected as one mound and no pits.



**Figure 20.** A charcoal kiln that is detected as one mound and three pits.



**Figure 21.** A charcoal kiln that is not detected by the present automatic methods.

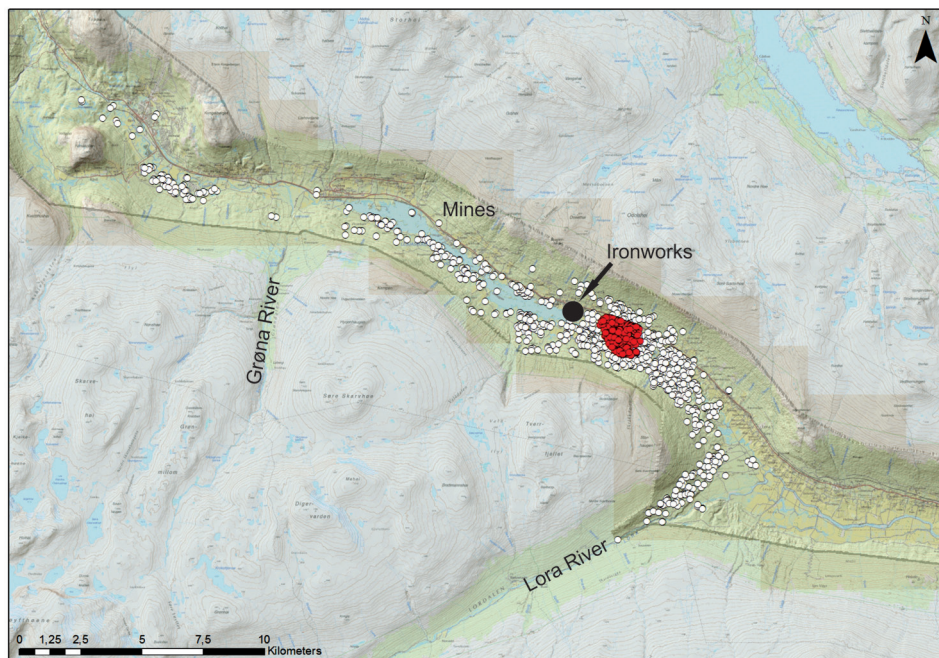


**Figure 22.** Overall map of the distribution of charcoal kilns surrounding Lesja Jernverk (ironworks). Field controlled kilns in red, visual inspection in white.

Schneider *et al.* (2015) recently attempted automatic detection of charcoal kilns in a large kiln field near Cottbus, Germany. These kilns have a somewhat different topographical expression than the kilns from Lesja, but many of the challenges in applying automatic detection are similar, e.g., the number of false detections.

The following resources were spent: the ALS data for the forested area of Lesja municipality cost about NOK 500,000, of which Oppland County paid NOK 150,000 in a cost-sharing agreement with other ALS data users; visual interpretation prior to field work amounted to about 40 man hours; field work 60 hours; and reporting 20 hours.

## 5. DISCUSSION AND CONCLUSIONS

The perceived success of using automatic detection methods depend on many factors. The most important seems to be how well the archaeological structures of interest stand out from the terrain in the DTM of the ALS ground points. We have experienced that archaeological pits in the form of pitfall traps in hunting systems and charcoal burning pits in iron extraction sites tend to stand out very well (Trier and Pilø, 2012). Natural pits of the same shape and size are rare in Norwegian landscapes. On the other hand, grave mounds are more easily confused with natural terrain features. The grave mounds



have a less distinct shape than the archaeological pits, many grave mounds are distorted, and there are many natural (partially) mound-like terrain features.

Still, the criterion for using automatic detection or not is if it is reducing the amount of work needed to create an accurate, detailed and complete archaeological mapping, suitable for modern land use planning.

The method for automatic mound detection seems to work better for a large grave field than for single grave mounds or small grave fields scattered over a large landscape. Although direct comparison of methods applied on different datasets is difficult, our present results for the Viking grave field at Vang, Oppdal are similar to those of Pregelbauer (2013) for the Birka-Hovgården grave field in Sweden. Our previous results for grave mounds in Vestfold County (Trier *et al.*, 2015) appear to be less convincing. However, the method did discover a grave field, consisting of 19 grave mounds, which had been overlooked by visual inspection of the DTM by experienced archaeologists. And by having each of the six confidence levels in a separate layer, one may use the 1-3 strongest confidence levels to identify interesting areas, and bring in detections with weaker confidence in the detailed mapping.

The detection results for charcoal kilns at Lesja demonstrated that some kilns may be detected as mounds, some may be indirectly detected as small pits along the edge, but many were missed. Since the charcoal kilns may have different shapes (Figure 23), depending on their state when abandoned, an automatic method may need to be tailored to detect a few different patterns. A charcoal kiln may have a flat or heap-shaped interior. It may have a (partly discontinuous) ditch or a number of (e.g., five) pits along the edge.

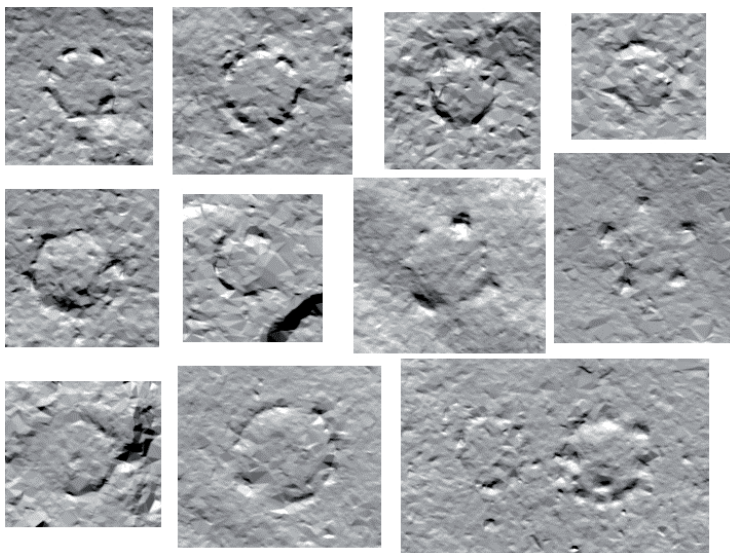


Figure 23. Charcoal kilns at Lesja iron works, Oppland County, Norway.

Although far from perfect, automatic detection is now used as part of the standard routine in detailed archaeological mapping in Vestfold and Oppland Counties. The current perspective is that automatic detection will not replace archaeologists, but is a useful tool for archaeologists in detailed mapping of cultural heritage. Our goal is to provide semi-automatic detection methods that are used by all 19 counties in Norway for detailed mapping of cultural heritage.

### **Acknowledgements**

This research was funded by the Directorate for Cultural Heritage in Norway (Riksantikvaren). We also thank the project partners for their dedicated involvement and enthusiasm. For more information on the project please visit: <https://www.nr.no/en/projects/cultsearcher>.

## BIBLIOGRAPHY

- Aurdal, L., Eikvil, L., Koren, H. and Loska, A. (2006): Semi-automatic search for cultural heritage sites in satellite images. In: *From Space to Place, Proceedings of the 2nd International Conference on Remote Sensing in Archaeology*, Rome, Italy, December 4-7, 2006, pp. 1-6.
- Berg, P. S. (1983): Lesja jernverks historie, del 1 (in Norwegian). *Lesja Historielags Årsskrift 1*, pp. 9-27.
- Berg, P. S. (1984): Lesja jernverks historie, del 2 (in Norwegian). *Lesja Historielags Årsskrift 2*, pp. 6-24.
- Berg, P. S. (1985): Lesja jernverks historie, del 3 (in Norwegian). *Lesja Historielags Årsskrift 3*, pp. 9-30.
- Berg, P. S. (1986): Lesja jernverks historie, del 4 (in Norwegian). *Lesja Historielags Årsskrift 4*, pp. 10-28.
- Bewley, R. H., Crutchley, S.P. and Shell, C.A. (2005): New light on an ancient landscape: lidar survey in the Stonehenge World Heritage Site. *Antiquity 79*, pp. 636-647.
- Bollandsås, O. M., Risbøl, O., Ene, L. T., Nesbakken, A., Gobakken, T. and Næsset, E. (2012): Using airborne small-footprint laser scanner data for detection of cultural remains in forests: an experimental study of the effects of pulse density and DTM smoothing. *Journal of Archaeological Science 39*, pp. 2733-2743.
- Doneus, M. (2013): Openness as visualization technique for interpretative mapping of airborne lidar derived digital terrain models. *Remote Sensing 5*, pp. 6427-6442.
- Farbregd, O. (1980): Gravfeltet på Vang. Hundre dekar oldtidshistorie på prestegarden. (In Norwegian.) *Bøgda vår 2*, Oppdal Historielag, pp. 4-14
- Farbregd, O. (1993): Menn, kvinner, graver og status. (In Norwegian.) *Bøgda vår 15*, Oppdal Historielag, pp. 67-80.
- Fløttum, A.L. (2004): *Små graver – store spørsmål. Et gløtt inn i jernalderens gravskikk på Vang i Oppdal*. (In Norwegian.) Master thesis. University of Tromsø, Norway.
- Jakobsen, S. (1997): Jernverkstiden i Norge og jernverket på Lesja. En historisk oversikt. (In Norwegian.) *Lesja Historielags Årsskrift 15*, pp. 37-74.
- Hesse, R. (2010): Lidar-derived local relief models – a new tool for archaeological prospection. *Archaeological Prospection 17*, p. 67-72.
- Kokalj, Ž., Zakšek, K. and Oštir, K. (2011): Application of sky-view factor for the visualization of historic landscape features in lidar-derived relief models. *Antiquity 79*, pp. 263-273.
- Pregesbauer, M. (2013): Object versus pixel – classification techniques for high-resolution airborne remote sensing data. In *Proceedings of the 10th International Conference on Archaeological Prospection*, Vienna, 29 May - 2 June 2013, pp. 200-202.
- Schneider, A., Takla, M., Nicolay, A., Raab, A. and Raab, Y. (2015): A template-matching approach combining morphometric variables for automated mapping of charcoal kiln sites. *Archaeological Prospection 22*(1), pp. 45-62.

- Trier, Ø. D., Larsen, S. Ø. and Solberg, R. (2009): Automatic detection of circular structures in high-resolution satellite images of agricultural land. *Archaeological Prospection* 16(1), pp. 1-15.
- Trier, Ø. D. and Pilø, L. H. (2012): Automatic detection of pit structures in airborne laser scanning data. *Archaeological Prospection* 19(2), pp. 103-121.
- Trier, Ø. D., Zorrea, M. and Tønning, C. (2015): Automatic detection of mound structures in airborne laser scanning data. *Journal of Archaeological Science: Reports* 2(1), pp. 69-79.